Synthesis and Properties of New Dialkoxyphenylene Quinoxaline-Based Donor-Acceptor Conjugated Polymers and Their Applications on Thin Film Transistors and Solar Cells

MEI-HSIU LAI,[1] CHU-CHEN CHUEH,[1] WEN-CHANG CHEN,[1,2] JYH-LIH WU,[3] FANG-CHUNG CHEN[3]

[1]Department of Chemical Engineering, National Taiwan University, Taipei 106, Taiwan

[2]Institute of Polymer Science and Engineering, National Taiwan University, Taipei 106, Taiwan

[3]Department of Photonics and Institute of Electro-optical Engineering, National Chiao Tung University, Hsinchu 300, Taiwan

Received 16 October 2008; accepted 20 November 2008
DOI: 10.1002/pola.23219
Published online in Wiley InterScience (www.interscience.wiley.com).

ABSTRACT: Synthesis, properties, and optoelectronic device applications of four new bis-[4-(2-ethyl-hexyloxy)-phenyl]quinoxaline(**Qx(EHP)**)-based donor-acceptor conjugated copolymers are reported, in which the donors are thiophene(**T**), dithiophene(**DT**), dioctylfluorene(**FO**), and didecyloxyphenylene(**OC10**). The optical band gaps (E_g) of **PThQx(EHP)**, **PDTQ(EHP)**, **POC10DTQ(EHP)**, and **PFODTQ(EHP)** estimated from the onset absorption are 1.57, 1.65, 1.77, and 1.92 eV, respectively. The smallest E_g of **PThQx(EHP)** among the four copolymers is attributed to the balanced donor/acceptor ratio and backbone coplanarity, leading to a strong intramolecular charge transfer. The hole mobilities obtained from the thin film transistor (TFT) devices of **PThQx(EHP)**, **PDTQ(EHP)**, **POC10DTQ(EHP)**, and **PFODTQ(EHP)** are 2.52×10^{-4}, 4.50×10^{-3}, 4.72×10^{-5}, and 9.31×10^{-4} $cm^2\ V^{-1}\ s^{-1}$, respectively, with the on-off ratios of 2.00×10^4, 1.89×10^3, 4.07×10^3, and 2.30×10^4. Polymer solar cell based on the polymer blends of **PFODTQ(EHP)**, **PThQx(EHP)**, **POC10DTQ(EHP)**, and **PDTQ(EHP)** with [6, 6]-phenyl C61-butyric acid methyl ester (PCBM) under illumination of AM1.5 (100 mW cm^{-2}) solar simulator exhibit power conversion efficiencies of 1.75, 0.92, 0.79, and 0.43%, respectively. The donor/acceptor strength, molecular weight, miscibility, and energy level lead to the difference on the TFT or solar cell characteristics. The present study suggests that the prepared bis[4-(2-ethyl-hexyloxy)-phenyl]quinoxaline donor-acceptor conjugated copolymers would have promising applications on electronic device applications.
 J Polym Sci Part A: Polym Chem 47: 973–985, 2009
Keywords: charge transfer; conjugated polymers; copolymerization; donor-acceptor; polycondensation; quinoxaline; solar cells; thin film transistor

INTRODUCTION

Donor-acceptor (D-A) copolymers have attracted significant scientific interest recently as their electronic and optoelectronic properties can be

Additional Supporting Information may be found in the online version of this article.

Correspondence to: W.-C. Chen (E-mail: chenwc@ntu.edu.tw)

Journal of Polymer Science: Part A: Polymer Chemistry, Vol. 47, 973–985 (2009)

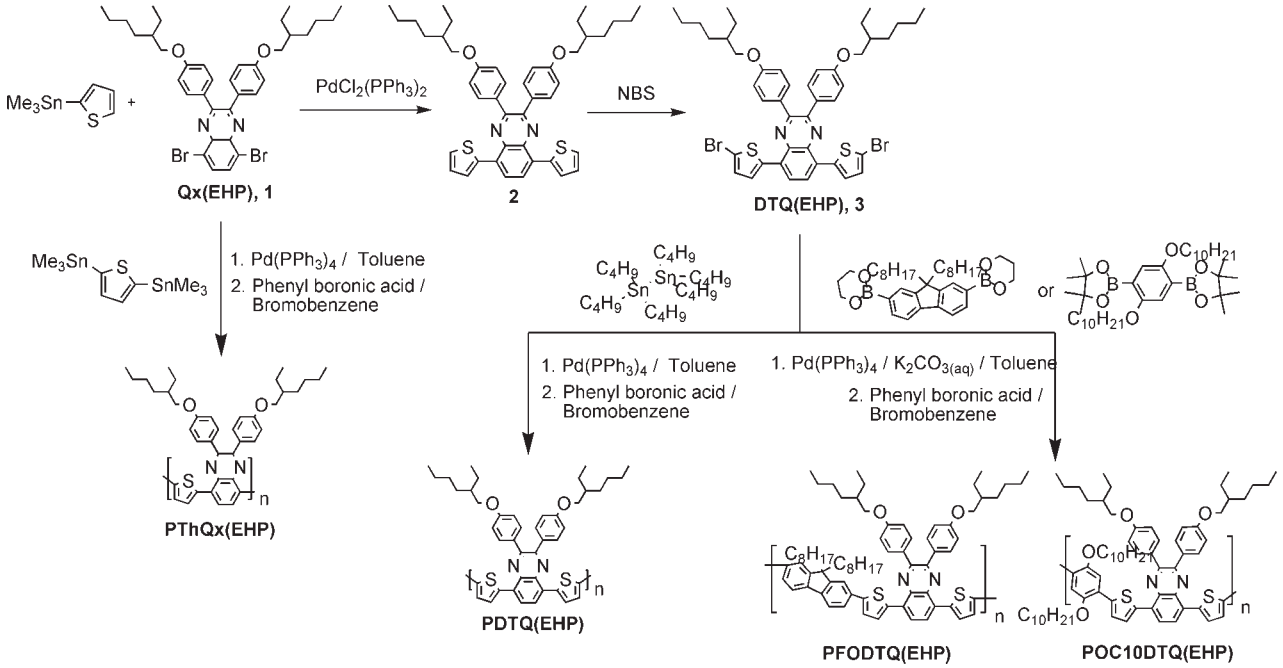

Scheme 1. Synthesis of **DTQ(EHP)**, **PThQx(EHP)**, **PDTQ(EHP)** and **PFODTQ (EHP)**, and **POC10DTQ(EHP)**.

manipulated through intramolecular charge transfer (ICT).[1–24] Such polymers may have potential applications in various organic electronic devices, such as light-emitting diodes,[3–8] field effect transistors,[9–16] and photovoltaic cells.[17–24]

Among D-A conjugated copolymers, the electron-donating moieties of fluorene,[3,5,14,15] thiophene,[13,25–29] dialkoxylphenylene,[30,31] and carbazole[32] have been reported. On the other hand, thieno[3,4-b]pyrazine (**TP**), 2,1,3-benzothiadiazole (**BT**), quinoxaline (**Q**), and pyridine (**Py**) are generally employed as the electron-accepting moieties. We are particularly interested in the quinoxaline-based copolymers due to their good charge-transfer characteristics and stability for device applications.[33–35] We found that poly(thiophene-*alt*-alkylquinoxaline)-based thin film transistor exhibited a medium high hole mobility with a relatively high on/off ratio[13] and ambipolar carrier transport by blending with poly(benzobisimidazophenanthroline).[16] A recent report by Ingänas's group demonstrated that fluorene-quinoxaline alternating copolymer exhibited a high power conversion photovoltaic efficiency due to its balanced electron and hole mobilities.[36] Another study by Scherf's group discovered the quinoxaline/ologothiophene copolymers having the unexpected independence of photophysical properties with the thiophene segment length.[26] We believe that the intramolecular charge transfer and backbone planarity played important roles on the aforementioned results.

In this article, we report the synthesis, properties, and device applications of bis-[4-(2-ethyl-hexyloxy)-phenyl]quinoxaline-based donor-acceptor conjugated copolymers, in which the donors include dioctylfluorene, didecyloxyphenylene, and thiophene. These polymers were synthesized by palladium(0)-catalyzed Suzuki or Stille coupling reaction, as shown in Scheme 1. The long bis[4-(2-ethyl-hexyloxy)-phenyl] side groups on the quinoxaline moiety significantly improve the polymer solubility for device applications. The effects of donor-acceptor strength and backbone planarity on the electronic and optoelectronic properties of the studied copolymers were investigated. Furthermore, field-effect carrier mobility obtained from the bottom gate thin film transistor was correlated with the polymer structure. Polymer solar cell devices fabricated by polymer/PCBM blends sandwiched between a transparent anode (ITO/PEDOT:PSS) and a cathode (Ca) were also explored. The present study revealed that the

new polymers had potential applications for flexible electronic devices.

EXPERIMENTAL

Materials

N-bromosuccinimide (NBS), tributyl(thien-2-yl)stannane, bis(triphenylphosphine)-dichloro palladium(II) [$(PPh_3)_2Cl_2Pd(II)$], 9,9-dioctylfluorene-2,7-diboronic acid bis(1,3-propanediol)ester, tetrakis (triphenylphosphine)-palladium(0) [$(PPh_3)_4$ Pd(0)], trioctylmethyl ammonium chloride (aliquat® 336), phenyl boronic acid, bromobenzene, and [6, 6]-phenyl C61-butyric acid methyl ester (PCBM) were purchased from Aldrich (Missouri, USA) or Acros (Geel, Belgium) and used without further purification. Ultra-anhydrous solvents and common organic solvents, such as THF and toluene, were purchased from Tedia (Ohio, USA).

The following monomers were prepared according to literature procedures: 4,4′-dihydroxybenzil,[37] 4,4′-bis(2-ethylhexyloxyl)benzyl,[38] 5,8-dibromo-2,3-bis-[4-(2-ethyl-hexyloxy)-phenyl]-quinoxaline **(Qx(EHP)**, **1)**,[39] 2,5-bis(trimethylstannyl) thiophene,[40] and 2,5-didecyloxyphenylene-1,4-bis-(4,4,5,5-tetramethyl-1,3,2-dioxaborolate) (**DP**).[31]

2,3-Bis(4-(2-ethylhexyloxy)phenyl)-5,8-dithien-2-yl-quinoxalines (2)

To a solution of **Qx(EHP)** (1.0 g, 1.43 mmol) and tributyl(thien-2-yl)stannane (1.59 g, 4.29 mmol) in toluene (10 mL), $(PPh_3)_2Cl_2Pd(II)$ (20 mg) was added. The mixture was refluxed for 24 h. After cooling to room temperature, the mixture was poured into methanol and the precipitate was filtered off. The crude product was dried under vacuum at 50 °C to obtained a brown-yellow powder (904 mg, yield: 90%). ^{1}H NMR (500 MHz, CD_2Cl_2) δ (ppm): 0.90–0.96 (12H, s, —CH_3), 1.34–1.54 (16H, br, —CH_2—), 1.74–1.75 (2H, s, —CH—), 3.91–3.92 (4H, s, —OCH_2—), 6.92–6.93 (4H, s, Ar—H), 7.19–7.20 (2H, s, Ar—H), 7.53–7.54 (2H, s, Ar—H), 7.70–7.72 (2H, s, Ar—H), 7.88 (2H, s, Ar—H), 8.14 (2H, s, Ar—H).

2,3-Bis(4-(2-ethylhexyloxy)phenyl)-5,8-bis[5′-bromo-dithien-2-yl-quinoxalines] (DTQ(EHP)), (3)

2,3-bis(4-(2-ethylhexyloxy)phenyl)-5,8-dithien-2-yl-quinoxalines (**2**) (1.35 g, 1.92 mmol) was dissolved in THF, and NBS (*N*-bromosuccinimide) (752 mg, 4.22 mmol) was immediately added. After the mixture was stirred at room temperature for 3 h, it was poured into methanol and the precipitate was filtered off. The crude product was dried under vacuum at 50 °C to obtain an orange powder (1.49 g, yield: 90%). ^{1}H NMR (500 MHz, CD_2Cl_2) δ (ppm): 0.91–0.98 (12H, s, —CH_3), 1.34–1.54 (16H, br, —CH_2—), 1.76 (2H, s, —CH—), 3.92 (4H, s, —OCH_2—), 6.94–6.96 (4H, s, Ar—H), 7.15 (2H, s, Ar—H), 7.60 (2H, s, Ar—H), 7.66 (2H, s, Ar—H), 8.10 (2H, s, Ar—H).

General Procedure of Polymerization

As shown in the Scheme 1, Stille coupling reaction was used to synthesize two thiophene/quinoxaline-based copolymers, **PThQx(EHP)** and **PDTQ(EHP)**. Monomers and $(PPh_3)_4Pd(0)$ were dissolved in toluene, and then the solution was stirred under nitrogen atmosphere and refluxed with vigorous stirring for 72 h. The end groups were capped by refluxing for another 12 h each with phenyl boronic acid and bromobenzene (both 1.0 equivalent with respect to the dibromo monomer). After cooling to room temperature, the resulting solution was dropped into a mixture of methanol and D.I. water. The precipitated solid was filtered and collected. The crude product was extracted in a Soxhlet apparatus with acetone for 24 h to remove the oligomer and catalyst residues. It was then dried under vacuum at 60 °C for 24 h to obtain the polymer product.

Suzuki cross-coupling reaction was used to synthesize **PDTQ(EHP)**, **POC10DTQ(EHP)**, and **PFODTQ(EHP)**, as shown in Scheme 1. Donor monomers (**DP** and fluorene), acceptor monomers **DTQ(EHP)**, and $(PPh_3)_4Pd(0)$ were dissolved in a mixture of toluene (15 mL) and aqueous 2 M K_2CO_3 (ca. 10 mL) with several drops of aliquat® 336. The following handling steps are all the same as described earlier in the Stille coupling reaction.

Poly[thiophene-2,5-diyl-alt-2,3-bis(4-(2-ethylhexyloxy)phenyl)-5,8-quinoxaline] (PThQx(EHP))

557 mg (0.8 mmol) of **Qx(EHP)** and 328 mg (0.8 mmol) of 2,5-bis(trimethylstannyl) thiophene were used to afford dark solid (270 mg, yield: 52%). ^{1}H NMR (500 MHz, CD_2Cl_2) δ (ppm): 0.88–0.92 (12H, s, —CH_3), 1.31–1.52 (16H, br, —CH_2—), 1.70–1.83 (2H, s, —CH—), 3.66–3.89 (4H, s, —OCH_2—), 6.77–6.89 (4H, s, Ar—H), 7.43–7.98 (8H, br, Ar—H). Anal. Calcd. for $C_{42}H_{52}N_2O_2S$

(%): C, 77.6; H, 7.5; N, 4.5; S, 5.2; O, 3.9. Found: C, 74.5; H, 7.1; N, 4.3; S, 6.3. Weight average molecular weight distribution (M_w) from gel-permeation chromatography (GPC) was 5040, with a polydispersity index (PDI) of 1.26.

Poly[2,3-bis(4-(2-ethylhexyloxy)phenyl)-5,8-dithien-2-yl-quinoxaline] (PDTQ(EHP))

688 mg (0.8 mmol) of **DTQ(EHP)** and 464 mg (0.8 mmol) of bis(tributyltin) were used to afford dark solid (400 mg, yield: 71%). ^{1}H NMR (500 MHz, CD_2Cl_2) δ (ppm): 0.69 (12H, s, —CH_3), 1.01–1.82 (18H, br, —CH2— and —CH—), 3.69–3.89 (4H, br, —OCH_2—), 5.72–8.04 (14H, br, Ar—H). Anal. Calcd. for $C_{44}H_{48}N_2O_2S_2$ (%): C, 75.4; H, 6.9; N, 4.0; S, 9.2; O, 4.6. Found: C, 71.9; H, 7.0; N, 3.5; S, 8.3. M_w and PDI from GPC were 11,560 and 1.68, respectively.

Poly[2,5-didecyloxy-1,4-phenylene-alt-2,3-bis[4-(2-ethylhexyloxy)phenyl)-5,8-dithien-2-yl-quinoxaline] (POC10DTQ(EHP))

688 mg (0.8 mmol) of **DTQ(EHP)** and 514 mg (0.8 mmol) of monomer **DP** were used to afford dark-purple solid (560 mg, yield : 63%). ^{1}H NMR (500 MHz, CD_2Cl_2) δ (ppm): 0.83–0.98 (18H, d, —CH_3), 1.22–1.88 (44H, br, —CH_2—), 1.93–1.65 (6H, d, —OC—CH_2— and —CH—), 3.90–4.18 (8H, q, —OCH_2—), 6.84–6.92 (4H, s, Ar—H), 7.20–8.16 (12H, br, Ar—H). Anal. Calcd. for $C_{70}H_{92}N_2O_4S_2$(%): C, 77.2; H, 8.5; N, 2.6; S, 5.9. Found: C, 77.0; H, 9.1; N, 2.4; S, 5.5. M_w and PDI from GPC were 14,350 and 1.67, respectively.

Poly[2,5-didecyloxy-1,4-phenylene-alt-2,3-bis(4-(2-ethylhexyloxy)phenyl)-5,8-dithien-2-yl-quinoxaline] (PFODTQ(EHP))

688 mg (0.8 mmol) of **DTQ(EHP)** and 447 mg (0.8 mmol) of 9,9-dioctylfluorene-2,7-diboronic acid bis(1,3-propanediol) ester were used to afford red solid (520 mg, yield: 58%). ^{1}H NMR (500 MHz, CD_2Cl_2) δ (ppm): 0.74 (6H, s, —CH_3), 0.95–1.09(d, 18H, —CH_3 and 24H, —CH_2—), 1.38–1.52 (16H, d, —CH_2—), 1.70–1.80 (2H, s, —CH—), 2.18 (4H, s, —CH_2—), 3.98 (4H, s, —OCH_2—), 6.80–7.01 (4H, s, Ar—H), 7.54–8.20 (16H, br, Ar—H). Anal. Calcd. for $C_{73}H_{88}N_2O_2S_2$ (%): C, 80.5; H, 8.1; N, 2.6; S, 5.9; O, 2.9. Found: C, 80.8; H, 8.6; N, 2.4; S, 5.6. M_w and PDI from GPC were 53,070 and 2.38, respectively.

Characterization

^{1}H NMR spectra were recorded by Bruker Avance DRX 500 MHz spectrometer in dichloromethane-d_2. Gel permeation chromatographic (GPC) analysis was performed on a Lab Alliance RI2000 instrument (one column, MIXED-D from Polymer Laboratories) connected with one refractive index detector from Schambeck SFD Gmbh. All GPC analyses were performed on polymer/THF solution at a flow rate of 1 mL/min at 40 °C and calibrated with polystyrene standards. Elemental analyses were performed with a Heraeus varioIII-NCSH instrument.

Thermal decomposition temperatures (T_d) of the prepared polymers were characterized by a TA instrument TGA 951 thermogravimetric analyzer (TGA) at a heating rate of 20 °C/min under a nitrogen atmosphere from room temperature to 800 °C, and differential scanning calorimetry (DSC) measurements were performed under a nitrogen atmosphere at a heating rate of 10 °C/min from 0 to 300 °C using a TA instrument DSC-910S.

The absorption spectra and photoluminescence (PL) spectra were recorded at room temperature with a Jasco model UV/VIS/NIR V-570 spectrometer and Fluorolog-3 spectrofluorometer (Jobin Yvon), respectively. For the solution spectra, polymers were dissolved in THF (ca. 1 mg/mL) and then put in a quartz cell for measurement. For the thin film spectra, polymers were first dissolved in $CHCl_3$ (ca. 10 mg/mL); then the solution spin-coated at a speed rate of 500 rpm for 20 s onto quartz substrate.

The electrochemical properties of the polymer films were investigated by a Bioanalytical System Model CV-27 potentiostat and a BAS X-Y recorder with a 0.1 M acetonitrile or DMF solution containing Tetrabutylammonium Perchlorate (TBAP) as the electrolyte. TBAP was obtained from commercial sales and recrystallized twice from ethyl acetate and then dried in vacuum prior to use. Platinum wire and ITO glass (polymer films area about 0.5 $\times$ 0.7 cm^2) were used as auxiliary and working electrodes, respectively, and the solution of the polymer in THF (ca. 1 mg/mL) was used to prepare the polymer film on ITO glass by drop coating. All cell potentials were taken with the use of an Ag/AgCl, KCl (sat.) reference electrode. Then, the cyclic voltammetry in films were examined by the three-electrode cell at a voltage scan rate of 0.1 V s. Furthermore, the reference electrode was calibrated through running the cyclic

voltammetry of ferrocene without any polymer film coated on ITO glass. The obtained potential values were then converted to versus ferrocene. The energy parameters EA and IP were estimated from the measured redox potentials on the basis of the prior works on conjugated polymers which have shown that: IP = (E^{ox}_{onset} + 4.8) and EA = (E^{red}_{onset} + 4.8), where the onset potentials are in volts (versus F_c+/F_c) and IP and EA are in electron volts.[41,42] The electronic structure parameters, HOMO and LUMO, were investigated with the relations of HOMO = −IP and LUMO = −EA by assuming no configuration interactions.

Polymer Thin Film Transistors

Polymer thin film transistor was fabricated with a bottom-contact and bottom-gate configuration on the heavily *n*-doped silicon wafers. The source/drain regions were defined by a 130 nm Au layer through a regular shadow mask, and the channel length (L) and width (W) were 25 and 500/1000 μm, respectively. A thermally grown 200 nm SiO_2 used as the gate dielectric with a capacitance of 68 nF cm^2. The aluminum was used to create a common bottom-gate electrode. Afterward, the substrate was modified with octyltrichlorosilane (OTS) coupling agent to promote the molecular chain ordering of the polymer semiconductor at the gate dielectric/semiconductor interface. 0.5 wt % polymer solution in chlorobenzene was filtered through 0.50-μm pore size PTFE membrane syringe filters, spin-coated at a speed rate of 1000 rpm for 60 s onto the silanized SiO_2/Si substrate and annealed at 100 °C overnight under vacuum. Output and transfer characteristics of the OTFT devices were measured using a Keithley 4200 semiconductor parametric analyzer. All the procedures and electronic measurements were performed in ambient air. The structures of polymer thin films on SiO_2/Si substrates were characterized by means of tapping mode atomic force microscopy (AFM) with a Nanoscope 3D controller (Digital Instruments, Santa Barbara, CA) at room temperature. Commercial silicon cantilevers (Nanosensors, Germany) with typical spring constants of 21–78 Nm^{-1} were used, and images were taken continuously with the scan rate of 0.8 Hz. The processing and annealing conditions of thin film of polymer samples are the same as the device fabrication to simulate the polymer transistor structures.

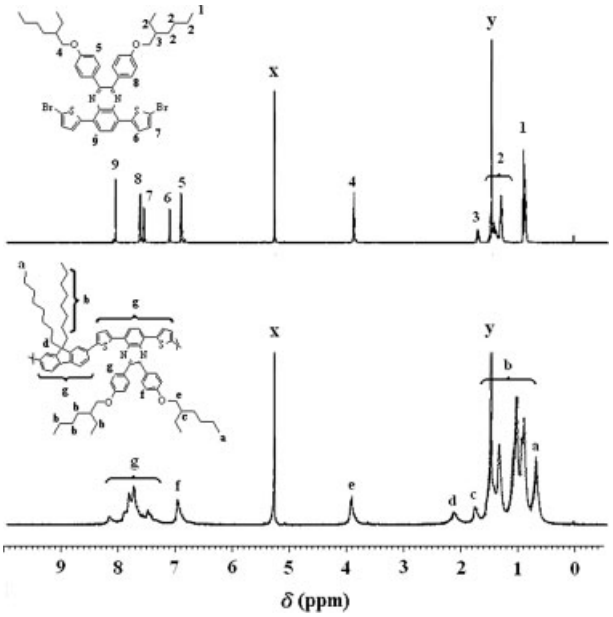

Figure 1. ^{1}H NMR spectra of **DTQ(EHP)** and **PFODTQ(EHP)** in CD_2Cl_2. Labels of x and y are CD_2Cl_2 and H_2O, respectively.

Polymer Solar Cells

Polymer solar cell devices were fabricated by spin-coating a blend of polymer/PCBM sandwiched between a transparent anode (ITO/PEDOT:PSS) and a cathode (Ca). First, PEDOT:PSS was spin-coated on the patterned ITO glass and then an active layer spin-coated (800 rpm) from the dichlorobenzene solution (∼ 0.8 wt %), followed by postannealing treatment at 110 °C. Then, Ca (30 nm) /Al (100 nm) was vapor deposited to serve as cathode. Keithley 2400 was used to measure the curves of current density versus voltage (J-V curves), and the efficiency was calculated under the 100 mW cm^{-2} simulated sunlight (AM 1.5G).

RESULTS AND DISCUSSION

Polymer Structure Characterization

Figure 1 shows the ^{1}H NMR spectra of monomer **(DTQ(EHP))** and the corresponding polymer **(PFODTQ(EHP))** in *d*-dichloromethane. For the spectrum of **DTQ(EHP)**, the signals in the ranges of 0.91–1.76 and 3.93 ppm are assigned to the protons of alkoxy group on the quinoxaline. The signals in 6.94–8.10 ppm are attributed to the protons on the quinoxaline and thiophene moieties. The ^{1}H-NMR spectrum of **PFODTQ(EHP)** shows

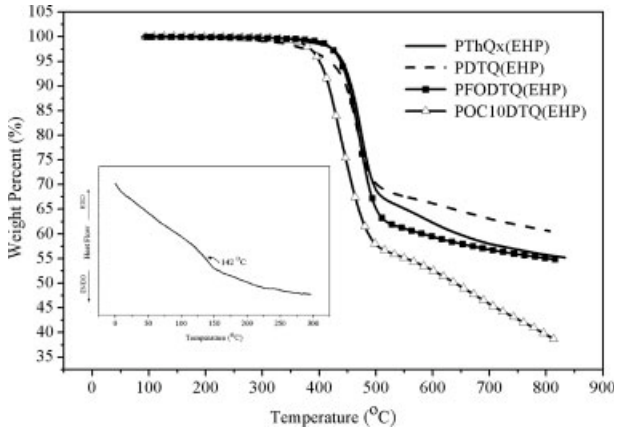

Figure 2. TGA curves of the four copolymers at a heating rate of 20 °C/min under nitrogen atmosphere. The insert shows the DSC curves of **PFODTQ(EHP)** at a heating rate of 10 °C/min under nitrogen atmosphere.

similar proton signal positions as those of **DTQ(EHP)** except the signals in 0.74–2.18 ppm due to the *n*-alkyl group on the fluorene moiety. The numbers of protons estimated from peak integration are in a fair agreement with the corresponding chemical structure of the copolymers. The ^{1}H spectra of other polymers (Supp. Info. Fig. S1) also agree well with the proposed polymer structures.

All the polymers are readily soluble in common organic solvents, such as THF, chloroform, DMF, and dichlorobenzene. The weight-averaged molecular weights (M_w) of the polymers determined by GPC are in the range of 5040–53,070 with PDI of 1.26–2.38. The low molecular weight of **PThQx(EHP)** is probably due to the low monomer reactivity by the Stille coupling reaction or the steric hindrance of the long 4-(2-ethylhexyloxy)phenylene group on the quinoxaline. The elemental analyses of the four copolymers are in a reasonable agreement with the theoretical estimation. The slightly larger deviation on the carbon and sulfur contents of **PThQx(EHP)** and **PDTQ(EHP)** could be due to the end group effect, since the two copolymers have low molecular weights.

Figure 2 shows TGA and DSC curves of the studied copolymers. The thermal decomposition temperatures (T_d, 95 wt % residue) of the four copolymers are in the range of 400–441 °C, indicating their good thermal stability. Among the four copolymers, only **PFODTQ(EHP)** shows a glass transition temperature (T_g) at 142 °C. The rigid backbone of the other three copolymers probably limits the chain motion and thus T_g is not observed.

Optical Absorption and Photoluminescence Properties

The UV–visible absorption spectra of the synthesized polymers in dilute THF solutions and thin films are shown in Figure 3, and their corresponding absorption maxima (λ_{max}^{abs}) are summarized in Table 1. The λ_{max}^{abs} of **PThQx(EHP)**, **PDTQ(EHP)**, **POC10DTQ(EHP)**, and **PFODTQ(EHP)** solutions in the visible region are observed at 566, 579, 536, and 524 nm, respectively, while those of polymer films at 612, 586, 576, and 538 nm. In comparison, the λ_{max}^{abs} are much more red-shifted than those of parent poly(quinoxaline),[1] polythiophene (nonregioregular),[1] polyfluorene[5] or poly(dioctylphenylene).[30] It suggests the significance of the intramolecular charge transfer between the donor and bis[4-(2-ethyl-hexyloxy)-phenyl]quinoxaline. The optical band gaps (E_g) of **PThQx(EHP)**, **PDTQ(EHP)**, **POC10DTQ**

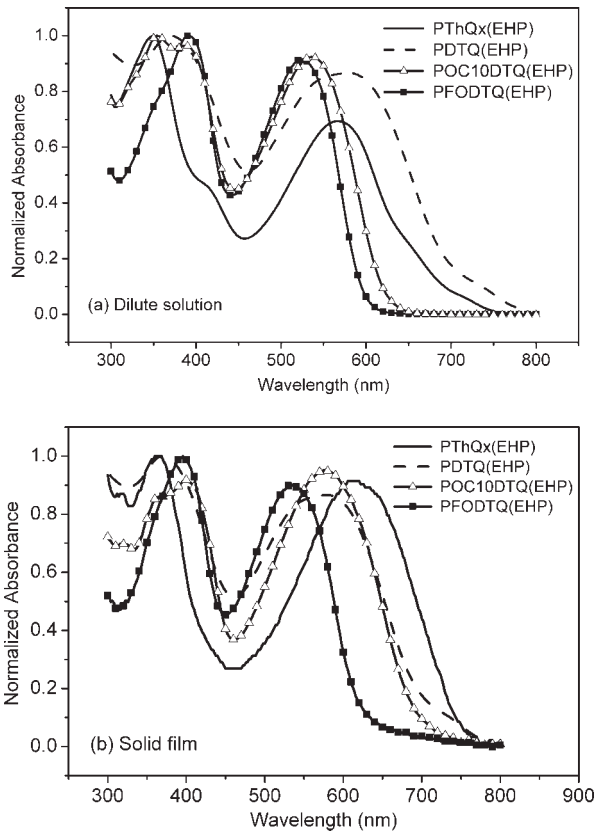

Figure 3. Normalized UV–visible spectra of the four copolymers in (a) dilute THF solutions and (b) solid films, respectively.

Table 1. Optical and Electrochemical Properties of **PThQx(EHP)**, **PDTQ(EHP)**, **POC10DTQ(EHP)**, and **PFODTQ(EHP)**

				Oxidation (vs F_c+/F_c)		Reduction (vs F_c+/F_c)		
	λ_{max}^{abs} (soln) (nm)[a]	λ_{max}^{abs} (film) (nm)	E_g^{opt} (eV)[b]	E_{onset} (V)	HOMO (eV)	E_{onset} (V)	LUMO (eV)	E_g^{elec} (eV)
PThQx(EHP)	350, 566	364, 612	1.57	0.22	−5.02	−1.70	−3.10	1.92
PDTQ(EHP)	366, 579	386, 586	1.65	0.23	−5.03	−1.70	−3.10	1.93
POC10DTQ(EHP)	356, 388[c], 536	368[c], 400, 576	1.77	0.18	−4.98	−1.84	−2.96	2.02
PFODTQ(EHP)	390, 524	396, 538	1.92	0.58	−5.38	−1.50	−3.30	2.08

[a] In THF dilute solution.
[b] Estimated from the absorption edge of the film.
[c] Emission shoulder.

(EHP), and **PFODTQ(EHP)** estimated by the onset absorption are 1.57, 1.65, 1.77, and 1.92 eV, respectively. **PThQx(EHP)** has a smaller E_g than **PDTQ(EHP)** since it has the more balanced donor-to-acceptor ratio (1:1) and leads to a higher intramolecular charge transfer. Such result is similar to that reported previously on the thiophene-thienopyrazine copolymers.[15] Furthermore, the unsubstituted thiophene moieties of **PDTQ(EHP)** are less bulky than the moieties of dioctylfluorene and didecyloxyphenylene in **POC10DTQ(EHP)** and **PFODTQ(EHP)**, respectively, which enhance the coplanarityof the polymer backbone and enlarge the polymer conjugation length. In summary, the lower E_g of **PDTQ(EHP)** than those of **POC10DTQ(EHP)** or **PFODTQ(EHP)** is probably resulted from the higher backbone coplanarity of the five-member thiophene moiety in comparison with the six-member phenylene ring.

The absorption spectra of **PThQx(EHP)** and **PDTQ(EHP)** show blue shifts compared with the *n*-octylbiphenyl substituted thiophene-quinoxaline copolymers[26] but red-shift in comparison with those of the alkyl-substituted copolymers.[1] It suggests that the significance of the side chain on the backbone planarity of thiophene-quinoxaline copolymers, which leads to the difference on the photophysical properties. The λ_{max}^{abs} of **PFODTQ(EHP)** film is similar to that of APFO-15 reported in the literature,[36] in which the APFO-15 has a *meta*-position substitution of dialkoxy group on the phenylene ring.

The normalized photoluminescence (PL) absorption spectra of the four copolymers in dilute THF solution and thin film are shown in Figure 4. The PL measurements are excited at the wavelength of 500–580 nm based on their optical absorption peaks. The λ_{max}^{PL} of **PThQx(EHP)**,

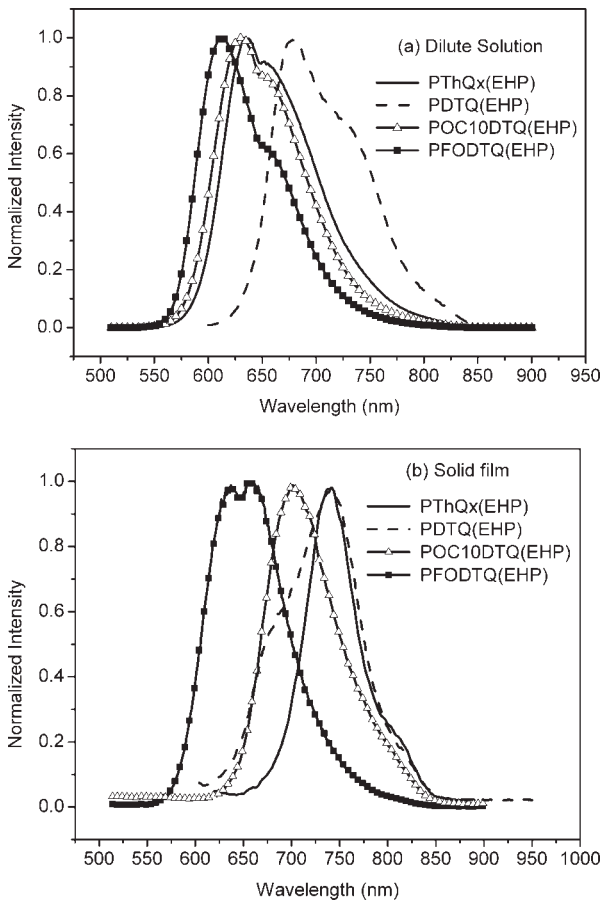

Figure 4. Normalized PL spectra of the four copolymers in (a) dilute THF solutions and (b) solid films, respectively.

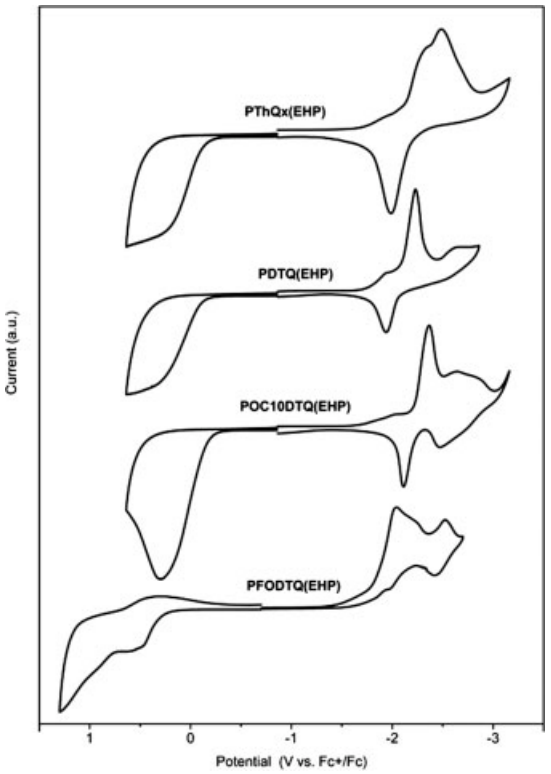

Figure 5. Cyclic voltammograms of the four polymer films on ITO glass at a scanning rate of 0.1 V s^{-1} in DMF/acetonitrile containing 0.1 M TBAP.

PDTQ(EHP), **POC10DTQ(EHP)**, and **PFODTQ(EHP)** in THF are 636, 678, 630, and 612 nm, respectively, while those in solid films are 740, 742, 702, and (636, 658) nm. The large red shifts of the λ_{max}^{PL} in the solid films compared with their solutions are probably resulted from the enhanced interchain interaction and thus promote energy transfer in the aforementioned polymer films.

Electrochemical Characteristics

The electrochemical characteristics of the four copolymers were investigated by cyclic voltammetry and summarized in Table 1. Figure 5 shows the cyclic voltammograms of the four polymer films. All of the prepared copolymers exhibit quasi-reversible reductive reaction but only **PFODTQ(EHP)** has a reversible oxidation. The LUMO levels of **PThQx(EHP)** and **PDTQ (EHP)** estimated from the onset reduction are −3.10 eV, with the HOMO potentials estimated from the onset oxidation in the range of −5.02 to −5.03 eV. It suggests that the HOMO/LUMO levels of the two polymers do not change significantly even though the thiophene content varies. Furthermore, the electrochemical band gaps of **PThQx(EHP)** and **PDTQ(EHP)** estimated from cyclic voltammetry (1.92 versus 1.93 eV) are very close. The LUMO levels of **POC10DTQ(EHP)** and **PFODTQ(EHP)** are −2.96 and −3.30 eV, respectively, with their HOMO levels are −4.98 and −5.38 eV. In comparison with the HOMO and LUMO levels of poly(9,9-octylfluorene) (PFO) at −5.6 and −2.0 eV,[31] the energy levels of **PFODTQ(EHP)** have been significantly varied due to the modulated ICT strength. The electrochemical band gaps are 0.2–0.4 eV larger than the corresponding optical ones, which is probably due to the exciton binding energy of conjugated polymers.[31] However, the trend between the polymer structure and the obtained band gap is similar.

Thin Film Transistor Characteristics

The charge transporting characteristics of the four polymers were explored by their bottom contact thin film transistor (TFT) devices and summarized in Table 2. Figure 6 shows the TFT characteristic curves of all four copolymers on the OTS-modified SiO_2. These polymers showed typical *p*-type I-V characteristics (drain current I_d versus drain voltage V_d at different gate voltages V_g) when operated in the accumulation mode

Table 2. TFT Characteristics of the Four Copolymers, **PThQx(EHP)**, **PDTQ(EHP)**, **POC10DTQ(EHP)**, and **PFODTQ(EHP)**

Polymer	Mobility ($Cm^2\ V^{-1}\ s^{-1}$)	On/Off	RMS (nm)
PThQx(EHP)	2.52×10^{-4}	2.00×10^4	1.68
PDTQ(EHP)	4.50×10^{-3}	1.89×10^3	1.96
POC10DTQ(EHP)	4.72×10^{-5}	4.07×10^3	0.61
PFODTQ(EHP)	9.31×10^{-4}	2.30×10^4	0.21

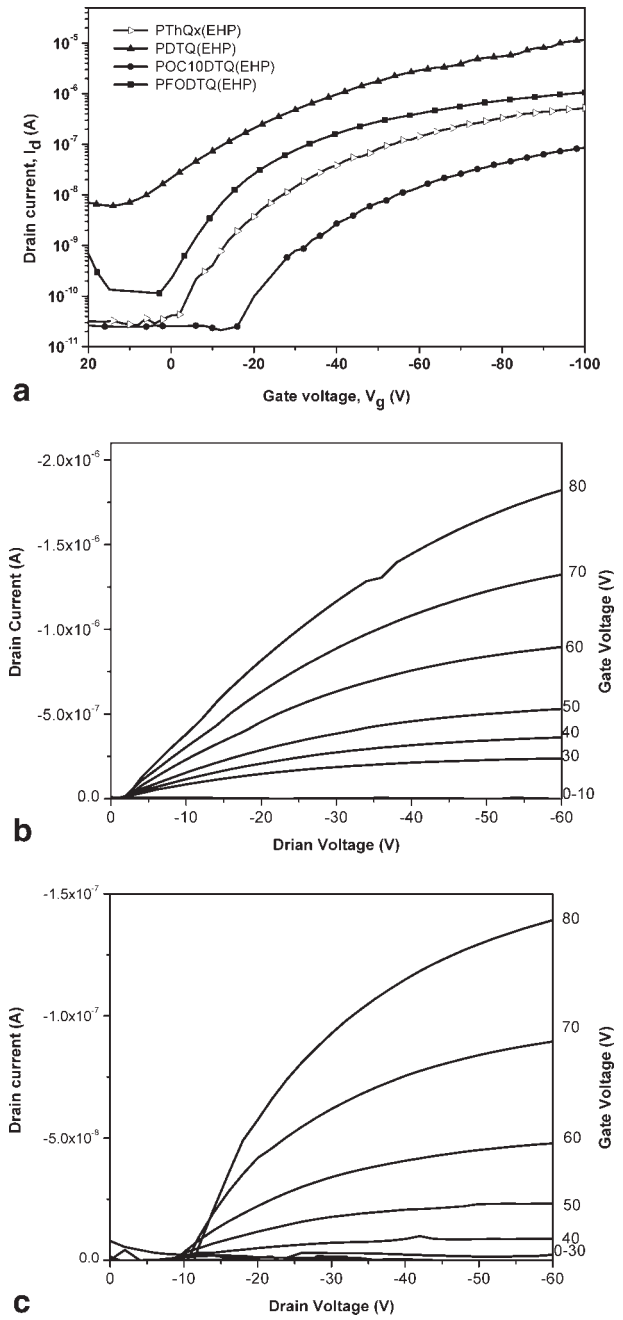

Figure 6. (a) Transfer characteristics of the polymer TFT devices with an OTS-modified surface and annealed at 100 °C, where $V_{ds} = -100$ V. (b) and (c) are the output characteristics of **PDTQ(EHP)** and **PDOC10DTQ(EHP)** based TFT devices.

operation. In the saturation region ($V_d > V_g - V_t$), I_d can be described by eq 1:

$$I_d = \frac{WC_o\mu_h}{2L}(V_g - V_t)^2 \quad (1)$$

Here, W and L are the channel width and length, respectively. C_o is the capacitance of the gate insulator per unit area (SiO_2, 200 nm, $C_o = 17$ nF cm^{-2}). The saturation region mobility of the studied polymers was calculated from the transfer characteristics involving plotting $(I_d)^{1/2}$ versus V_g. The estimated hole mobilities of **PThQx(EHP)** and **PDTQ(EHP)** are 2.52×10^{-4} and 4.50×10^{-3} cm^2 V^{-1} s^{-1}, respectively, with the corresponding on-off ratios of 2.00×10^4 and 1.89×10^3 in the ambient conditions. Both of them possess similar threshold voltage (V_T) around -17 V, but **PDTQ(EHP)** shows a significantly higher *p*-channel mobility as compared to **PThQx(EHP)**. It may be attributed to the larger molecular weight of **PDTQ(EHP)** than that of **PThQx(EHP)**. In addition, the estimated hole mobility of **POC10DTQ(EHP)** and **PFODTQ (EHP)** are 4.72×10^{-5} and 9.31×10^{-4}, respectively, with the corresponding on-off ratios of 4.07×10^3 and 2.30×10^4. Processing solvent plays an important role on the resulted surface structured of semiconducting polymers and their TFT mobilities.[43] However, the surface morphologies of these two polymers are smooth and without significant aggregation, as shown in Figure 7. It indicates that the polymer structure leads to the difference on the carrier mobility. Even though the molecular weights of **POC10DTQ(EHP)** and **PFODTQ (EHP)** are much higher than **PDTQ(EHP)**, the hole mobilities of **POC10DTQ(EHP)** and **PFODTQ(EHP)** are still lower than that of **PDTQ(EHP).** It indicates the importance of intramolecular charge transfer on the TFT mobility. By annealing above the T_g of **PFODTQ (EHP)**, its mobility is slightly improved to 1.30×10^{-3} cm^2 V^{-1} s^{-1}, which could be realized through the insignificant variation of polymer surface morphology, as shown in Supporting Information (Supp. Info. Fig. S3).

Characterization of Polymer Solar Cells

Photovoltaic devices were fabricated from polymer/PCBM blends of a sandwiched structure composed of a transparent anode (ITO/PEDOT:PSS) and a cathode (Ca). The photovoltaic properties of the four copolymers are summarized in Table 3. Figure 8 shows the current-voltage (J-V) characteristics of the aforementioned device measured under illumination of AM1.5 (100 mW cm^{-2}) solar simulator. Although different blend ratios (1:1, 1:2, and 1:4) of copolymer to PCBM are used, only the power conversion efficiency (PCE) of **PFODTQ (EHP)** increases at a higher PCBM content. For

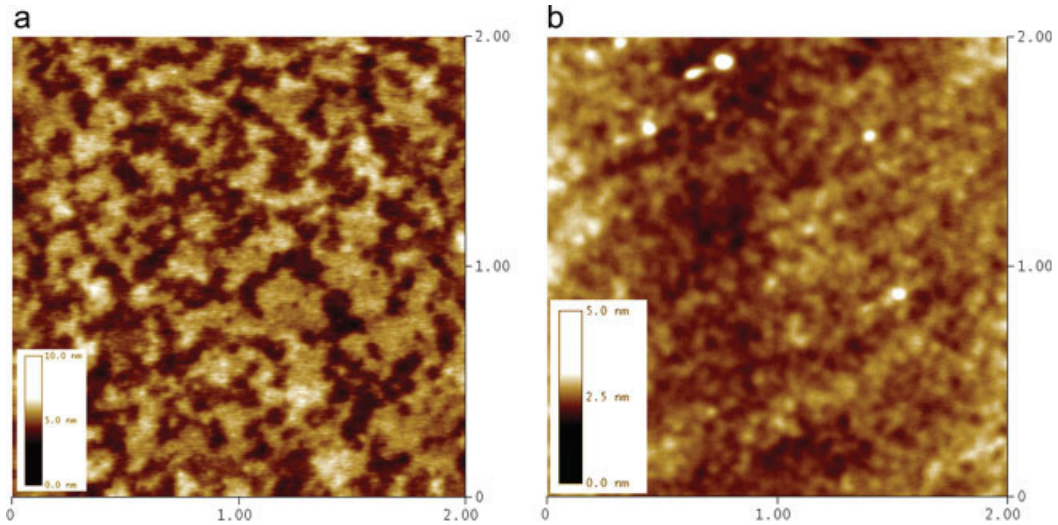

Figure 7. AFM tapping mode topographical images of (a) **POC10DTQ(EHP)** and (b) **PFODTQ(EHP)** thin films on the SiO_2/Si substrate.

example, power conversion efficiency (PCE) of **PThQx(EHP)**/ PCBM decreases from 0.92% of 1:1 ratio to 0.65% of 1:2 ratio, and 0.51% of 1:4 ratio. In comparison, the PCE of the **PFODTQ (EHP)**/PCBM with the ratios of 1:1, 1:2, and 1:4 are 1.16, 1.24, and 1.75%, respectively. Such variation of the copolymer/PCBM ratio with PCE is attributed to the formation of charge transfer exciton, which leads to the higher hole mobility of the fluorine-based copolymers at a larger PCBM content.[36,44–46]

The PCE of the **PThQx(EHP)**, **PDTQ(EHP)**, and **POC10DTQ(EHP)** with the 1:1 blend ratio to PCBM are 0.92, 0.43, and 0.79%, respectively. The I_{sc} of **POC10DTQ(EHP)** is relatively small, possibly due to its lowest hole mobility among the four copolymers. Comparing **PDTQ(EHP)**, **PThQx(EHP)** shows a relatively higher PCE than **PDTQ(EHP)** despite its low molecular weight. It may be explained by their surface structures shown in Figure 9. As shown in the figure, the surface of **PThQx(EHP)** is homogeneous with a smaller root mean square (RMS) roughness of 2.54 nm. However, **PDTQ(EHP)** has a large RMS roughness of 10.67 nm, probably from the PCBM aggregation (white part). The low miscibility between the **PDTQ(EHP)** and PCBM explains its poor solar cell characteristics. As shown in Table 3, the open-circuit voltage (V_{oc}) of **PFODTQ(EHP)** reached as large as 0.79 V, which may be resulted from the relatively low HOMO energy level (−5.14 eV) of **PFODTQ (EHP)** compared with the other copolymers (ca. −4.8 eV). V_{oc} is an approximate measure of the difference between the oxidation potentials of the donor polymer and the reduction potential of PCBM. Furthermore, the good film quality (due to high M_w) and medium high hole mobility are

Table 3. Polymer Solar Cell Characteristics of the Four Copolymers, **PThQx(EHP)**, **PDTQ(EHP)**, **POC10DTQ(EHP)**, and **PFODTQ(EHP)**

Polymer	Polymer:PCBM ratio	V_{oc} (V)	I_{sc} (mA cm^{-2})	FF	PCE (%)
PThQx(EHP)	1:1	0.69	2.91	0.46	0.92
PDTQ(EHP)	1:1	0.39	2.24	0.49	0.43
POC10DTQ(EHP)	1:1	0.67	3.02	0.39	0.79
PFODTQ(EHP)	1:1	0.73	4.48	0.36	1.16
	1:2	0.75	4.29	0.39	1.24
	1:4	0.79	6.05	0.37	1.75

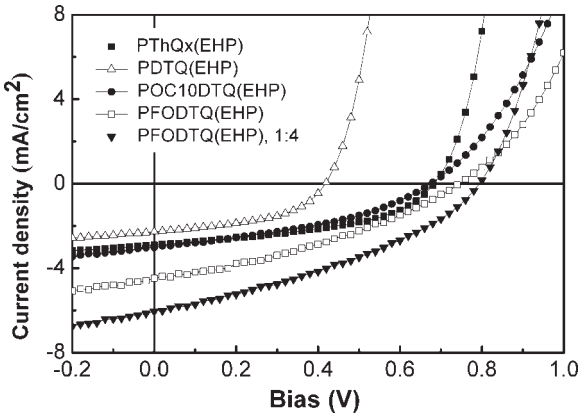

Figure 8. J-V characteristics of polymer solar cells using polymer/PCBM blends under the illumination of AM 1.5G, 100 mW cm^{-2}. The ratio of polymer/PCBM is 1:1 except **PFODTQ(EHP)** with both the ratios of 1:1 and 1:4.

probably contributed to good short-circuit current (I_{sc}) of **PFODTQ(EHP)**. The photocurrent increased at a higher PCBM loading provides the formation of adequate electron and hole percolation paths and leads to efficient charge collection to the electrodes.[36] The PCE of **PFODTQ(EHP)** device reaches 1.75% based on the aforementioned optimization. Although the PCE of **PFODTQ(EHP)** is lower than that of similar polymer with 3.5%,[36] it could be improved through device optimization.

CONCLUSIONS

In this study, we have successfully synthesized four quinoxaline-based donor-acceptor copolymers for thin film transistor (TFT) and solar cell applications. **PThQx(EHP)** has the smallest band gap of 1.57 eV among the four copolymers due to a strong intramolecular charge transfer. The hole mobilities obtained from the TFT devices of the four copolymers are in the range of 4.72×10^{-5}–4.50×10^{-3} cm^2 V^{-1} s^{-1} with the on-off ratios of 1.89×10^3 to 2.30×10^4. Polymer solar cells based on the blend of copolymer with PCBM blend exhibit power conversion efficiencies of 0.43–1.75%. The donor/acceptor strength, molecular weights, miscibility, and energy level lead to the difference on the TFT or solar cell characteristics. The electronic and optoelectronic properties suggest that the prepared bis[4-(2-ethyl-hexyloxy)-phenyl] quinoxaline-containing copolymers would have potential applications for electronic devices.

The financial supports of National Science Council (NSC96-2221-E-002-021), Excellent Research Projects of National Taiwan University, and Ministry of

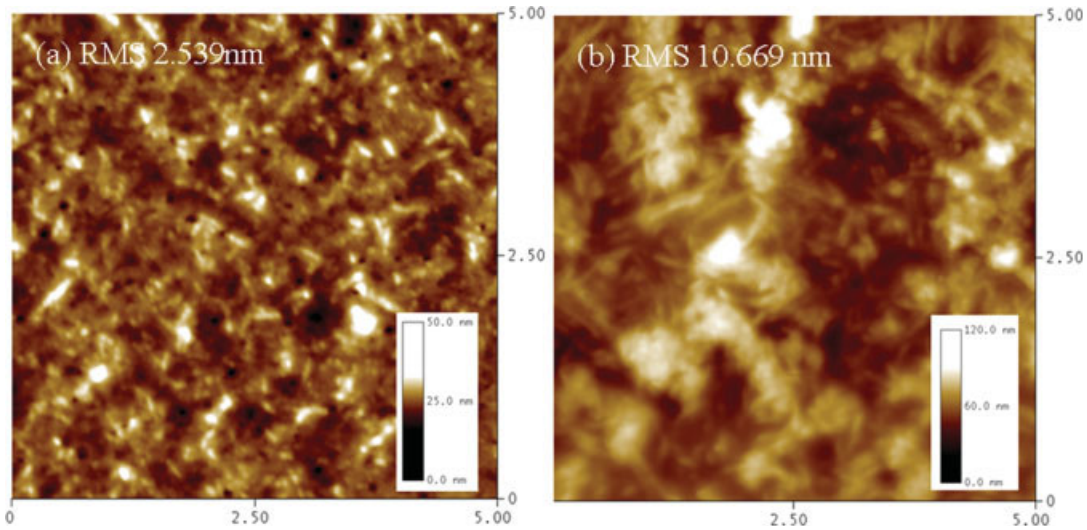

Figure 9. AFM tapping mode topographical images of (a) **PThQx(EHP)**/PCBM and (b) **PDTQ(EHP)**/PCBM blends on ITO glass coating with PEDOT:PSS. [Color figure can be viewed in the online issue, which is available at www.interscience.wiley.com.]

Economic Affairs of Taiwan (96-Ec-17-A-08-S1-015) are highly appreciated.

REFERENCES AND NOTES

1. Yamamoto, T.; Zhou, Z. H.; Kanbara, T.; Shimura, M.; Kizu, K.; Maruyama, T.; Nakamura, Y.; Fukuda, T.; Lee, B. L.; Ooba, N.; Tomaru, S.; Kurihara, T.; Kaino, T.; Kubota, K.; Sasaki, S. J Am Chem Soc 1996, 118, 10389–10399.
2. Yamamoto, T.; Lee, B. L.; Kokubo, H.; Kishida, D.; Hirota, K.; Wakabayashi, T.; Okamoto, H. Macromol Rapid Commun 2003, 24, 440–443.
3. Ego, C.; Marsitzky, D.; Becker, S.; Zhang, J.; Grimsdale, A. C.; Mullen K.; MacKenzie, J. D.; Silva, C.; Friend, R. H. J Am Chem Soc 2003, 125, 437–443.
4. Yang, R. Q.; Tian, R. Y.; Yan, J. G.; Zhang, Y.; Tang, J.; Hou, Q.; Yang, W.; Zhang, C.; Cao, Y. Macromolecules 2005, 38, 244–253.
5. Wu, W. C.; Liu, C. L.; Chen, W. C. Polymer 2006, 47, 527–538.
6. Liu, J.; Guo, X.; Bu, L. J.; Xie, Z. Y.; Cheng, Y. X.; Geng, Y. H.; Wang, L. X.; Jing, X. B.; Wang, F. S. Adv Funct Mater 2007, 17, 1917–1925.
7. Liu, Y.; Cao, H.; Li, J.; Chen, Z.; Cao, S.; Xiao, L.; Xu, S.; Gong, Q. J Polym Sci Part A: Polym Chem 2007, 45, 4867–4878.
8. Liao, L.; Cirpan, A.; Chu, Q.; Karasz, F. E.; Pang, Y. J Polym Sci Part A: Polym Chem 2007, 45, 2048–2058.
9. Yang, Y.; Heeger, A. J. Nature 1994, 372, 344–346.
10. Sirringhaus, H.; Tessler, N.; Friend, R. H. Science 1998, 280, 1741–1744.
11. Babel, A.; Jenekhe, S. A. J Am Chem Soc 2003, 125, 13656–13657.
12. Dang, T. T. M.; Park, S. J.; Park, J.-W.; Chung, D.-S.; Park, C. E.; Kim, Y.-H.; Kwon, S.-K. J Polym Sci Part A: Polym Chem 2007, 45, 5277–5284.
13. Champion, R. D.; Cheng, K. F.; Pai, C. L.; Chen, W. C.; Jenekhe, S. A. Macromol Rapid Commun 2005, 26, 1835–1840.
14. Lee, W. Y.; Cheng, K. F.; Wang, T. F.; Chueh, C. C.; Chen, W. C.; Tuan, C. S.; Lin, J. L. Marcomol Chem Phys 2007, 208, 1909–1927.
15. Cheng, K. F.; Liu, C. L.; Chen, W. C. J Polym Sci Part A: Polym Chem 2007, 45, 5872–5883.
16. Babel, A.; Zhu, Y.; Cheng, K.-F.; Chen, W.-C.; Jenekhe, S. A. Adv Funct Mater 2007, 17, 2542–2549.
17. Dennler, G.; Scharber, M. C.; Ameri, T.; Denk, P.; Forberich, K.; Waldauf, C.; Brabec, C. J. Adv Mater 2008, 20, 579–583.
18. Tang, W.; Kietzke, T.; Vemulamada, P.; Chen, Z. K. J Polym Sci Part A: Polym Chem 2007, 45, 5266–5276.
19. Egbe, D. A. M.; Nguyen, L. H.; Schmidtke, K.; Wild, A.; Sieber, C.; Guenes, S.; Sariciftci, N. S. J Polym Sci Part A: Polym Chem 2007, 45, 1619–1631.
20. Shin, W. S.; Kim, S. C.; Lee, S. J.; Jeon, H. S.; Kim, M. K.; Naidu, B. V. K.; Jin, S. H.; Lee, J. K.; Lee, J. W.; Gal, Y. S. J Polym Sci Part A: Polym Chem 2007, 45, 1394–1402.
21. Kim, Y.; Cook, S.; Tuladhar, S. M.; Choulis, S. A.; Nelson, J.; Durrant, J. R.; Bradley, D. D. C.; Giles, M.; Mcculloch, I.; Ha, C. S.; Ree, M. Nat Mater 2006, 5, 197–203.
22. Huo, L.; He, C.; Han, M.; Zhou, E.; Li, Y. J Polym Sci Part A: Polym Chem 2007, 45, 3861–3971.
23. Zhang, F.; Mammo, W.; Andersson, L. M.; Admassie, S.; Andersson, M. R.; Ingnas, O. Adv Mater 2006, 18, 2169–2173.
24. Hadipour, A.; de Boer, B.; Wildeman, J.; Kooistra, F. B.; Hummelen, J. C.; Turbiez, M. G. R.; Wienk, M. M.; Janssen, R. A. J.; Blom, P. W. M. Adv Funct Mater 2006, 16, 1897–1903.
25. Scherf, U.; List, E. W. Adv Mater 2002, 14, 477–487.
26. Tsami, A.; Bunnagel, T. W.; Farrell, T.; Scharber, M.; Choulis, S. A.; Brabec, C. J.; Scherf, U. J. Mater Chem 2007, 17, 1353–1355.
27. Yamamoto, T.; Yasuda, T.; Sakai, Y.; Aramaki, S. Macromol Rapid Commun 2005, 26, 1214–1217.
28. Yasuda, T.; Yamamoto, T. Macromolecules 2003, 36, 7513–7519.
29. Jung, I. H.; Jung, Y. K.; Lee, J.; Park, J. H.; Woo, H. Y.; Lee, J. I.; Chu, H. Y.; Shim, H. K. J Polym Sci Part A: Polym Chem 2008, 46, 7148–7161.
30. Liu, C. L.; Tsai, J. H.; Lee, W. Y.; Chen, W. C.; Jenekhe, S. A. Macromolecules 2008, 41, 6952–6959.
31. Zhu, Y.; Champion, R. D.; Jenekhe, S. A. Macromolecules 2006, 39, 8712–8719.
32. Blouin, N.; Michaud, A.; Gendron, D.; Wakim, S.; Blair, E.; Neagu-Plesu, R.; Belletete, M.; Durocher, G.; Tao, Y.; Leclerc, M. J Am Chem Soc 2008, 130, 732–742.
33. Tsami, A.; Yang, X. H.; Farrell, T.; Neher, D.; Holder, E. J Polym Sci Part A: Polym Chem 2008, 46, 7794–7808.
34. Huo, L.; Tan, Z.; Wang, X.; Zhou, Y.; Han, M.; Li, Y. J Polym Sci Part A: Polym Chem 2008, 46, 4038–4049.
35. Udum, Y. A.; Yildiz, E.; Gunbas, G.; Toppare, L. J Polym Sci Part A: Polym Chem 2008, 46, 3723–3731.
36. Gadisa, A.; Mammo, W.; Andersson, L. M.; Admassie, S.; Zhang, F.; Andersson, M.; Ingänas, O. Adv Funct Mater 2007, 17, 3836–3842.

37. Moylan, C. R.; Miller, R. D.; Twieg, R. J.; Betterton, K. M.; Lee, V. Y.; Matray, T. J.; Nguyen, C. Chem Mater 1993, 5, 1499–1508.
38. Pisula, W.; Dierschke, F.; Müllen, K. J. Mater Chem 2006, 16, 4058–4064.
39. Mammo, W.; Admassie, S.; Gadisa, A.; Zhang, F.; Inganas, O; Andersson, M. Sol Energy Mater Sol Cells 2007, 91, 1010–1018.
40. Seitz, D. E.; Lee, S.-H.; Hanson, R. N.; Bottaro, J. C. Synth Commun 1983, 13, 121–128.
41. Li, Y. F.; Cao, Y.; Gao, J.; Wang, D. L.; Yu, G.; Heeger, A. J. Synth Met 1999, 99, 243–248.
42. Sun, Q. J.; Wang, H. Q.; Yang, C. H.; Li, Y. F. J Mater Chem 2003, 13, 800–806.
43. Yang, H.; Shin, T. J.; Yang, L.; Cho, K.; Ryu, C. Y.; Bao, Z. Adv Funct Mater 2005, 15, 671–767.
44. Mihailetchi, V. D.; Koster, L. J. A.; Blom, P. W. M.; Melzer, C.; de Boer, B.; van Duren, J. L. J.; Janssen, R. A. J Adv Funct Mater 2005, 15, 795–801.
45. Andersson, M.; Inganäs, O. Appl Phys Lett 2006, 88, 082103.
46. Gadisa, A.; Wang, X.; Admassie, S.; Per, E.; Oswald, F.; Langa, F.; Andersson, M. R.; Inganäs, O. Org Electron 2006, 7, 195–204.